

Magnetic and Electronic Properties of the New Ferrimagnet $\text{Sr}_8\text{CaRe}_3\text{Cu}_4\text{O}_{24}$

Masanori Kohno, Xiangang Wan and Xiao Hu

Computational Materials Science Center, National Institute for Materials Science, Tsukuba 305-0047, Japan

(Dated: October 27, 2018)

Magnetic and electronic properties of the recently-discovered material $\text{Sr}_8\text{CaRe}_3\text{Cu}_4\text{O}_{24}$ were investigated by means of a quantum Monte Carlo simulation, the Green function method and the LSDA+ U (local spin-density approximation plus the Hubbard- U term) method. The LSDA+ U calculation shows that the ground state is an insulator with magnetic moment $M=1.01\mu_B/\text{f.u.}$, which is consistent with experimental results. The magnetic sites were specified and an effective model for the magnetic properties of this compound derived. The resultant effective model is a three-dimensional Heisenberg model with spin-alternation. Finite-temperature properties of this effective model are investigated by the quantum Monte Carlo method (continuous-time loop algorithm) and the Green function method. The numerical results are consistent with experimental results, indicating that the model is suitable for this material. Using the analysis of the effective model, some predictions for the material are made.

I. INTRODUCTION

Strong electronic correlations produce a rich variety of phenomena. High- T_c superconductivity[1] is one of such a phenomenon. It is widely believed that the origin of high- T_c superconductivity is related to the nature of undoped systems[2], which are Mott insulators with an antiferromagnetic order. Recently-discovered perovskite cuprate $\text{Sr}_8\text{CaRe}_3\text{Cu}_4\text{O}_{24}$ [3] is a magnetic insulator which has spontaneous magnetization at room temperature and in some respects resembles parent materials of high- T_c superconductors. It is expected that the ferromagnetism of $\text{Sr}_8\text{CaRe}_3\text{Cu}_4\text{O}_{24}$ might be caused by strong electronic correlations due to a similar mechanism to the antiferromagnetism of parent materials of high- T_c superconductors. Furthermore, among ferromagnetic cuprates this material has an unusually high magnetic transition temperature (T_c) up to 440K, although those of other ferromagnetic cuprates are at most 30K[4]. Thus, the material is interesting for its high T_c induced by strong electronic correlations. The purpose of this paper is to clarify the origin of magnetism and to predict the possible magnetic properties of this material.

II. LOCAL SPIN-DENSITY APPROXIMATION

The lattice structure is shown in Fig. 1, which is determined experimentally[3]. In order to investigate electronic properties of the compound, the local spin-density approximation plus the Hubbard- U term (LSDA+ U) method using the package WIEN2K[5] which is an implementation of the density-functional APW-lo method[6], has been used. The cutoff values were set at $RK_{\text{max}}=7$, the LSDA+ U parameters $U=10\text{eV}$ and $J_{\text{LSDA}+U}=1.2\text{eV}$ [7]. For the exchange correlation, the standard generalized gradient approximation (GGA)[8] has been applied. The numerical results show that the ground-state is an insulator with a ferrimagnetic order: The charge gap is estimated as about 1.68eV. Magnetic moments are almost localized at Cu sites, and their di-

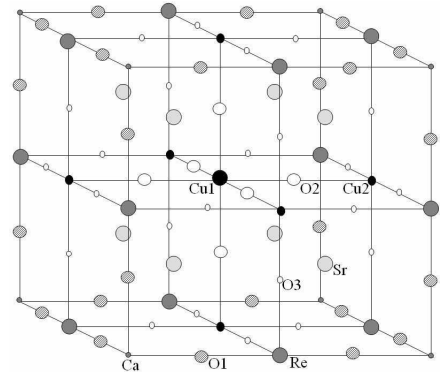


FIG. 1: Unit cell of $\text{Sr}_8\text{CaRe}_3\text{Cu}_4\text{O}_{24}$.

rections at Cu1 and Cu2 sites are opposite. The absolute values of the magnetic moments at Cu1 and Cu2 are $1.01\mu_B$ and $0.86\mu_B$ per formula unit (f.u.), respectively, and those of other sites are less than $0.07\mu_B/\text{f.u.}$. The total magnetic moment is $1.01\mu_B/\text{f.u.}$, which is comparable to the experimental result ($0.95\mu_B/\text{f.u.}$)[3]. The LSDA+ U calculation shows that the orbital degrees of freedom are also ordered. The high T_c would be due to the large overlap between orbitals of O2 and Cu originated from orbital ordering. The mechanism of the antiferromagnetic coupling is the super-exchange[9] as in the parent materials of high- T_c superconductors. Details of the LSDA+ U calculation are presented in a separate paper[10].

III. EFFECTIVE MODEL FOR MAGNETISM

By using LSDA+ U method, the magnetic sites of this compound have been identified. Since the system is an insulator, it is natural to expect that the effective model for magnetism is a Heisenberg model. It was assumed that the spins on nearest-neighbor sites interact with each other. Then, the Hamiltonian of the effective model is

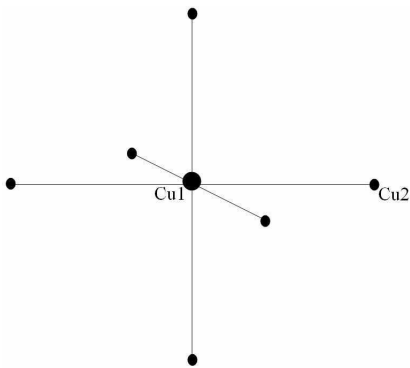


FIG. 2: Unit cell of the effective model.

expressed as

$$\mathcal{H} = J \sum_{i,p} \mathbf{S}_i \cdot \mathbf{s}_{i+\frac{p}{2}}, \quad (1)$$

where \mathbf{S}_i and $\mathbf{s}_{i+p/2}$ denote spin operators at Cu1 (i) and Cu2 ($i+p/2$) sites, respectively. Here, p represents the unit vectors ($p=\pm\hat{x}, \pm\hat{y}, \pm\hat{z}$). The unit cell of this effective model is illustrated in Fig. 2.

Consider the appropriate combination of spin length (S, s), where S and s denote the spin length at Cu1 and Cu2 sites, respectively. In order to determine these, the magnetization of the ground state (M_{GS}) and that of the fully-polarized state (M_{FP}) for the effective model in a unit cell were calculated. In the case of $(S, s)=(1/2, 1/2)$, $M_{\text{GS}}=1$ and $M_{\text{FP}}=2$, which correspond to $2\mu_{\text{B}}$ /f.u. and $4\mu_{\text{B}}$ /f.u., by setting the g -factor 2. For $(S, s)=(1/2, 1), (1, 1/2), (1, 1), (M_{\text{GS}}, M_{\text{FP}})$ becomes $(5/2, 7/2), (1/2, 5/2), (2, 4)$, respectively. Here, M_{GS} and M_{FP} obtained by the LSDA+ U method are $1.01\mu_{\text{B}}$ /f.u. and $5\mu_{\text{B}}$ /f.u.. Hence, $(S, s)=(1, 1/2)$ is the most suitable for this compound.

It should be noted that M_{GS} and M_{FP} of the effective model are exactly $1/2$ and $5/2$ (equal to $1\mu_{\text{B}}$ /f.u. and $5\mu_{\text{B}}$ /f.u.) in any size of systems due to the Marshall-Lieb-Mattis theorem[11]. The ground-state magnetization of the effective model ($1\mu_{\text{B}}$ /f.u.) is comparable to the experimental results[3].

Next, the strength of antiferromagnetic coupling J was considered. The energy difference between the ground state and the fully-polarized state in a unit cell was calculated by the exact diagonalization method. The result is $8J$. The energy difference was calculated for $\text{Sr}_8\text{CaRe}_3\text{Cu}_4\text{O}_{24}$ also by the LSDA+ U method. The result was $0.036Ry$. Hence, by comparing these results, $J=0.0045Ry(=710\text{K})$ was obtained.

IV. GREEN FUNCTION METHOD

Using the above arguments, the effective model for magnetism of $\text{Sr}_8\text{CaRe}_3\text{Cu}_4\text{O}_{24}$, which is a spin-alternating Heisenberg model in three-dimensions has

been obtained. In order to investigate finite-temperature properties of this compound, the Green function method[12] was applied to the effective model where Green functions are defined as Fourier components of time-dependent correlation functions:

$$G^{Ss}(k, \omega) = \frac{1}{N} \int dt \sum_{i,j} \langle\langle S_i^+(t); s_{j+\frac{p}{2}}^- \rangle\rangle e^{ik(r_i - r_{j+\frac{p}{2}}) - i\omega t}, \quad (2)$$

where N is the number of unit cells. Since there are four sites in a unit cell, $16(=4 \times 4)$ Green functions are necessary. Here, the double-bracket correlation function is defined as

$$\langle\langle A(t); B \rangle\rangle \equiv -\theta(t) \langle [A(t), B] \rangle. \quad (3)$$

Coupled equations were obtained for 16 Green functions by using a decoupling approximation[13]

$$\langle\langle S^z(t) s^+(t); s^- \rangle\rangle \simeq \langle S^z \rangle \langle s^+(t); s^- \rangle. \quad (4)$$

These equations were solved analytically and the temperature dependence of magnetizations was obtained using these Green functions by following Callen's scheme[14]. Figure 3 (a) shows the result of the Green function method. The agreement with the experimental result is good, indicating that the effective model is suitable for describing the magnetic properties of $\text{Sr}_8\text{CaRe}_3\text{Cu}_4\text{O}_{24}$. From the LSDA+ U result, J was set as $J=710\text{K}$.

V. QUANTUM MONTE CARLO SIMULATION

In order to investigate magnetic properties of this compound more quantitatively, a quantum Monte Carlo method was applied to the effective model. The algorithm used was the continuous-time loop algorithm (see Refs. in [15]), which is a powerful method for non-frustrated spin systems. More than one million updates for each simulation were performed. The system size was up to $16 \times 16 \times 16$ unit cells which correspond to 16,384 sites.

Spontaneous magnetization can be obtained by extrapolating $\bar{S}(N)$ which is defined as $\bar{S}(N, T) \equiv \sqrt{3 \langle S_0^z S_l^z \rangle_T}$, where S_0^z and S_l^z are the z -component of Cu1-spin at the center of the system and that of the furthest site from the center, respectively. Here, N denotes the number of unit cells. By extrapolating $\bar{S}(N, T)$ in the thermodynamic limit, we obtain the temperature dependence of spontaneous magnetization as shown in Fig. 3 (b). The quantum Monte Carlo result is consistent with experimental results. By tuning J to fit the transition temperature, we obtain $J=695\text{K}$. The first estimation of $J=710\text{K}$ based on LSDA+ U results was not far from the fitted value, suggesting that the above mapping is valid. To date, the temperature dependence of the spontaneous magnetization is the only quantity that has been measured experimentally[3]. However, since the effective model for this compound has been derived, further predictions of

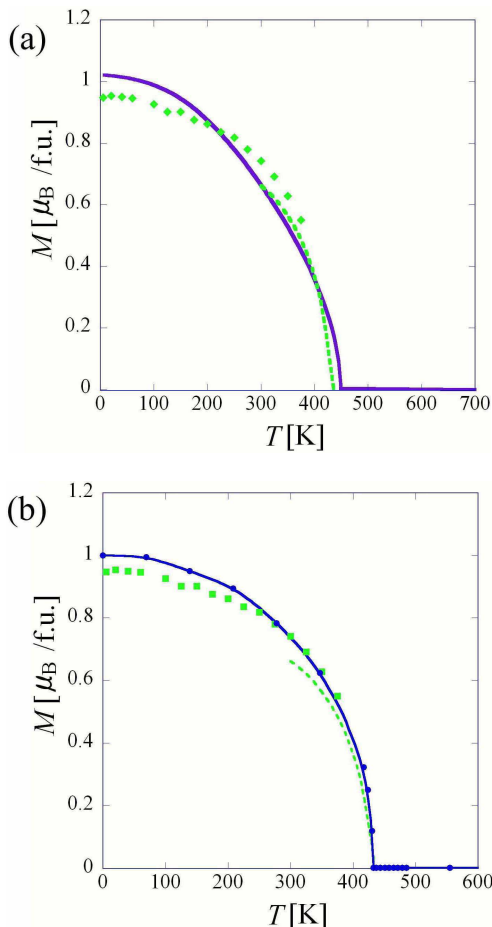


FIG. 3: Temperature dependence of spontaneous magnetization obtained by (a) the Green function method and (b) the quantum Monte Carlo method (solid curves). Dots and dotted line denote the experimental results[3].

its magnetic properties through the investigation of this effective model can be made.

The temperature dependence of the inverse of uniform and staggered susceptibilities above the critical temperature is shown in Fig. 4. As is evident from this figure, both susceptibilities diverge toward the critical point. In general, physical quantities show a power-law behavior at the critical point of the second-order phase transition. The universality class is characterized by the exponents of physical quantities such as length scale $\xi \propto \Delta T^{-\nu}$, magnetization $M \propto |\Delta T|^\beta$ and susceptibility $\chi \propto \Delta T^{-\gamma}$, where $\Delta T \equiv T - T_c$. In finite-size systems, the magnetization and the susceptibility can be expressed in terms of scaling functions as[16]

$$M \simeq |\Delta T|^\beta \bar{M}(L|\Delta T|^\nu), \quad (5)$$

$$\chi \simeq \Delta T^{-\gamma} \bar{\chi}(L\Delta T^\nu), \quad (6)$$

where L is the number of unit cells in the x -, y - or z -direction. $M|\Delta T|^{-\beta}$ and $\chi\Delta T^\gamma$ were plotted as a function of $L|\Delta T|^\nu$ in Fig. 5, where we use the exponents of

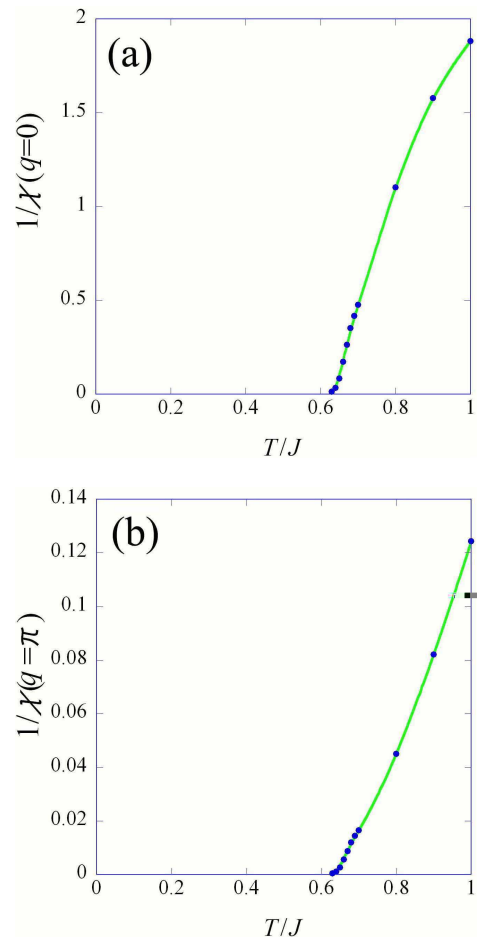


FIG. 4: Temperature dependence of the inverse of uniform (a) and staggered susceptibilities (b) above the critical temperature.

the three-dimensional (3D) Heisenberg model: $\nu=0.7054$, $\beta=0.3646$ and $\gamma=1.3866$ [17]. The figure shows that data in various sizes and various temperatures near the critical point fall into single curves, suggesting that the universality class is that of the 3D Heisenberg model.

The temperature dependence of the specific heat is plotted in Fig. 6. The size dependence of the specific heat is small. The maximum value is almost saturated at about 3.1. The critical temperature was estimated as 0.622 ± 0.002 , assuming that the specific heat is a maximum at the critical temperature. Since the specific heat has little size-effect, it is expected that the specific heat at the critical temperature remains finite in the thermodynamic limit. This is consistent with the scaling property of the 3D Heisenberg model: $C \propto \Delta T^{-\alpha}$, $\alpha = -0.1162 < 0$ [17].

VI. CONCLUSIONS

The magnetic and electronic properties of $\text{Sr}_8\text{CaRe}_3\text{Cu}_4\text{O}_{24}$ have been investigated by means

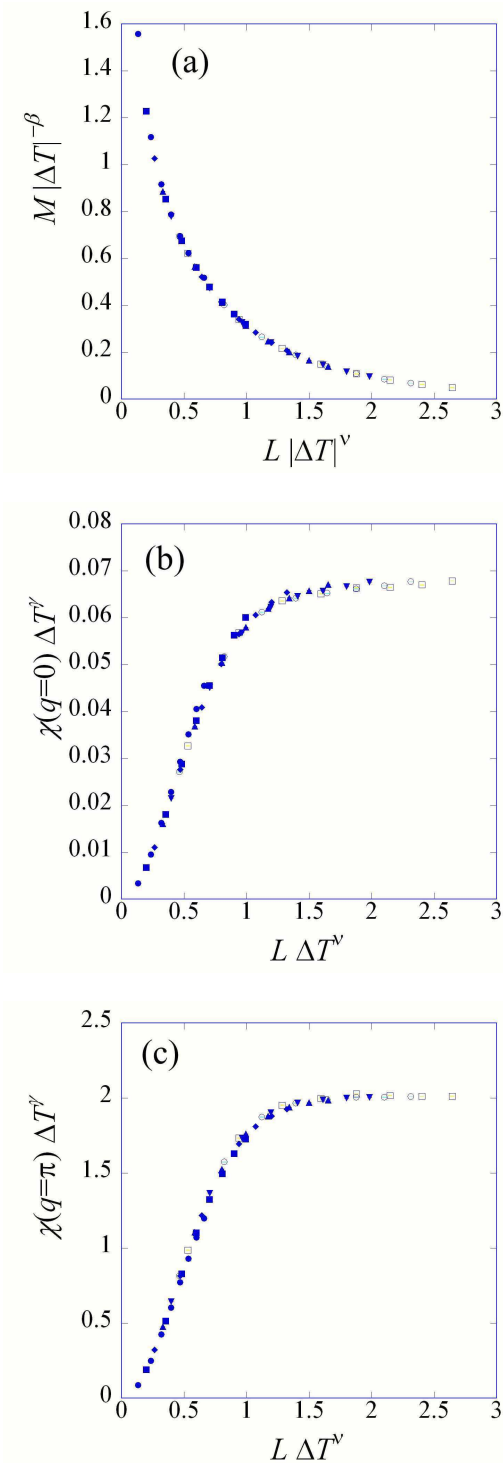


FIG. 5: Scaling plot for M and χ . We set the exponents of the three-dimensional (3D) Heisenberg model: $\nu=0.7054$, $\beta=0.3646$ and $\gamma=1.3866$ [17]. The data are obtained in clusters of $L=4\sim 16$ in the temperature range of $T/J=0.63\sim 0.7$.

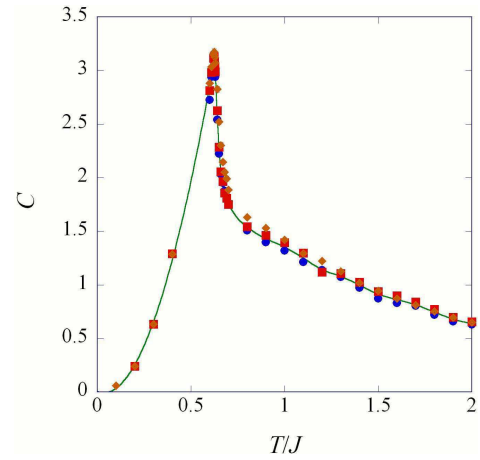


FIG. 6: Temperature dependence of the specific heat. Circles, squares and diamonds denote the data of $L=12, 14$ and 16 , respectively. Solid line is a guide to the eye.

of the quantum Monte Carlo method, the Green function method and the LSDA+ U method. Since the LSDA+ U calculation shows that magnetic moments are localized at Cu sites, a Heisenberg model was introduced as an effective model for magnetic properties. The spin lengths at Cu1 and Cu2 sites as one and one half, respectively, were obtained by comparing the result given by the effective model in a unit cell and that given by the LSDA+ U method. The finite-temperature properties of the effective model were investigated by the Green function method and the quantum Monte Carlo method. The agreement on magnetization at finite temperatures between the numerical results and the experimental results was good, suggesting that the effective model is suitable for describing the magnetic properties of $\text{Sr}_8\text{CaRe}_3\text{Cu}_4\text{O}_{24}$. The properties of the effective model were further investigated and revealed that the universality class of the critical point is that of the 3D Heisenberg model. Some of the results given by the effective model may be accessible by experiments.

Acknowledgements

Thanks are expressed to Dr. E. Takayama-Muromachi for drawing attention to this material and for valuable discussions. Dr. C. Yasuda, Dr. M. Arai and Dr. M. Katakiri are appreciated for technical help and thanks are due to Dr. A. Tanaka for discussions. This work was partially supported by Japan Society for the Promotion of Science (Grant-in-Aid for Scientific Research (C) No. 15540355).

[1] J.G. Bednorz and K.A. Muller, *Zeit. Phys. B* **64** (1986) 189.

[2] F.C. Zhang and T.M. Rice, *Phys. Rev. B* **37** (1988) 3759.

- [3] E. Takayama-Muromachi, T. Drezen, M. Isobe, N.D. Zhigadlo, K. Kimoto, Y. Matsui and E. Kita, *J. Solid State Chem.* **175** (2003) 366.
- [4] F. Mizuno, H. Masuda, I. Hirabayashi, S. Tanaka, M. Hasegawa and U. Mizutani, *Nature* **345** (1990) 788; I. Yamada, *J. Phys. Soc. Jpn.* **33** (1972) 979; K. Kohn, K. Inoue, O. Horie and S. Akimoto, *J. Solid State Chem.* **18** (1976) 27.
- [5] P. Blaha, K. Schwarz, G. Madsen, D. Kvasnicka and J. Luitz, WIEN2K, *An Augmented Plane Wave + Local Orbitals Program for Calculating Crystal Properties*, Karlheinz Schwarz, Tech. Universität Wien, Austria, 2001, ISBN 3-9501031-1-2.
- [6] E. Sjöstedt, L. Nordström and D.J. Singh, *Solid State Commun.* **114** (2000) 15; G.K.H. Madsen, P. Blaha, K.H. Schwarz, E. Sjöstedt and L. Nordström, *Phys. Rev. B* **64** (2001) 195134.
- [7] V.I. Anisimov, M.A. Korotin, I.A. Nekrasov, Z.V. Pchelkina and S. Sorella, *Phys. Rev. B* **66** (2002) 100502.
- [8] J.P. Perdew, K. Burke and M. Ernzerhof, *Phys. Rev. Lett.* **77** (1996) 3865.
- [9] H.A. Kramers, *Physica* **1** (1934) 182; P.W. Anderson, *Phys. Rev.* **115** (1959) 2.
- [10] X. Wan, M. Kohno and X. Hu, *Phys. Rev. Lett.* **94** (2005) 087205.
- [11] W. Marshall, *Proc. Roy. Soc. A* **232** (1955) 48; E.H. Lieb and D. Mattis, *J. Math. Phys.* **3** (1962) 749.
- [12] N.N. Bogolyubov and S.V. Tyablikov, *Dokl. Acad. Nauk. SSSR* **126** (1959) 53 [*Sov.Phys.Dokl.* **4** (1959) 604].
- [13] S.V. Tyablikov, *Ukr. Mat. Zh.* **11** (1959) 287.
- [14] H.B. Callen, *Phys. Rev.* **130** (1963) 890.
- [15] H.G. Evertz, *Adv. Phys.* **52** (2003) 1.
- [16] V. Privman and M.E. Fisher, *Phys. Rev. B* **30** (1984) 322.
- [17] J.C. Le Guillou and J. Zinn-Justin, *Phys. Rev. Lett.* **39** (1977) 95.